HSSJ (2009) 5: 51–57
DOI 10.1007/s11420-008-9096-1

ORIGINAL ARTICLE

Differences in Tendon Graft Healing Between the Intra-articular and Extra-articular Ends of a Bone Tunnel

Asheesh Bedi, MD · Sumito Kawamura, MD · Liang Ying, BVS · Scott A. Rodeo, MD

Received: 20 September 2008/Accepted: 14 October 2008/Published online: 4 December 2008

Abstract The basic biology of healing between a tendon graft and bone tunnel remains incompletely understood. Distinct variability in the morphological characteristics of the healing tendon–bone attachment site has been reported. We hypothesized that spatial and temporal differences in tendon-to-bone healing exist at different regions of a surgically created bone tunnel. Twenty-four male, Sprague–Dawley rats underwent anterior cruciate ligament (ACL) reconstruction in the left knee using a flexor digitorum longus tendon graft secured using suspensory periosteal fixation. Animals were sacrificed at 4, 7, 11, 14, 21, and 28 days after surgery and prepared for routine histology and immunohistochemical analysis of the healing enthesis at the intra-articular aperture (IAA), mid-tunnel, and extra-articular aperture (EAA). Six animals were used to measure mineral apposition rate (MAR) along the healing bone tunnel by double fluorochrome labeling at 14 and 28 days after surgery. The total area of calcified bone matrix was assessed with von Kossa staining and Goldner-Masson trichrome staining, respectively. The healing tendon–bone interface tissue exhibited a wide chondroid matrix at the IAA, in contrast to a narrow, fibrous matrix at the EAA. There were significantly more osteoclasts at the IAA compared to EAA throughout the study period, except 4 days after surgery ($p<0.05$). Collagen continuity between the tendon graft and bone tunnel increased over time, with a more parallel orientation and increased collagen fiber continuity between tendon and bone at the EAA compared to the IAA. MAR was also significantly greater at the EAA at 4 weeks ($p<0.001$). Significant differences in healing between the tendon graft and bone exist along the length of bone tunnel secured with suspensory fixation. The etiology of these differences is likely multifactorial in nature, including variable biological and biomechanical environments at different ends of the tunnel. Understanding these differences may ultimately allow surgeons to improve the quality of graft fixation and long-term outcomes after ACL reconstruction.

Keywords bone tunnel · anterior cruciate ligament · biology · tendon–bone healing

A. Bedi, MD · S. Kawamura, MD · L. Ying, BVS
Laboratory for Soft Tissue Research,
Hospital For Special Surgery,
535 East 70th Street, New York City, NY 10021, USA

S. A. Rodeo, MD (✉)
Section of Shoulder & Sports Medicine,
Laboratory for Soft Tissue Research,
Hospital for Special Surgery,
535 East 70th Street, New York City, NY 10021, USA
e-mail: rodeos@hss.edu

Introduction

The healing of tendon-to-bone is a basic requirement for the long-term survival of an anterior cruciate ligament (ACL) reconstruction. A tendon graft used for ACL reconstruction may be fixed with an interference screw in the bone tunnel at the joint entrance ("aperture fixation") or fixed outside of the tunnel at the exits ("suspensory fixation"). Whether suspensory or aperture fixation is employed, however, the weakest link following reconstruction is not the graft itself but rather the fixation points until graft osteointegration occurs [1–4]. Current techniques of ACL reconstruction all require some degree of tendon-to-bone healing in a surgically created bone tunnel. There are no analogous sites in humans where a native tendon passes through a bone tunnel, however, and the biology of this unique healing process remains incompletely understood.

Wide variations in the morphological characteristics of the tendon–bone attachment site after ACL reconstruction have been reported [5–23]. Some studies have demonstrated the formation of a native, direct type of insertion with an intermediate fibrocartilage zone at the interface. However, other studies have reported a fibrous tissue interface devoid of intervening fibrocartilage with tendon attached to bone by perpendicular collagen bundles [5–23]. No prior studies, however, have defined the differences in the tendon–bone healing response that may occur at different ends of a bone

tunnel. We hypothesize that such differences exist due to variable biological and biomechanical environments at opposing ends of a bone tunnel. In the current study, we use a rat model of ACL reconstruction using suspensory graft fixation to evaluate the spatial and temporal differences in the morphology of the healed tendon–bone attachment at different regions of a bone tunnel. We hypothesize that the healing enthesis at the extra-articular aperture will exhibit less interface scar tissue, improved collagen fiber organization and continuity, and increased new bone formation compared to the tendon–bone interface at the intra-articular aperture of the tunnel.

Methods

This study used an ACL reconstruction model in the left knee of skeletally mature, male Sprague–Dawley rats. The rats were obtained from a licensed US Department of Agriculture dealer and were housed in the Center for Laboratory Animal Services at our institution, in accordance with the standards established by the National Institutes of Health for the care and use of laboratory animals. This study was approved by the Institutional Animal Care and Use Committee.

Twenty-four male Sprague–Dawley rats (275–350 g) underwent unilateral ACL reconstruction. The procedure was performed on the left lower limb of a rat which had been anesthetized via intraperitoneal injection of a ketamine–xylazine cocktail solution. The full length of the flexor digitorum longus tendon was harvested through a small posteromedial ankle incision and midline plantar foot incision. The tendon was stripped of any attached muscle, and two 4-0 Ethibond stay sutures were placed, one in each end of the tendon. A medial parapatellar arthrotomy was made, and the anterior cruciate ligament was sectioned and removed in its entirety. Under direct visualization, the knee was flexed 60° to 70°, and a Keith needle (1.2 mm diameter) was used to drill a bone tunnel through the proximal tibia, penetrating the joint at the native ACL insertion footprint. Using a transtibial drilling technique, the Keith needle is drilled to create the femoral tunnel, starting at the native ACL origin and exiting at the proximal lateral femoral condyle. The Keith needle was used to pull the stay sutures in the proximal end of the flexor digitorum longus autograft tendon through the bone tunnels. The graft was pretensioned manually and secured to the surrounding periosteum outside the femoral followed by tibial tunnel, respectively, using 4-0 Ethibond suture with the knee maintained at 60° of flexion. The arthrotomy and skin incisions were closed in a standard, layered fashion. All animals were allowed ad libitum activity postoperatively.

Three animals were sacrificed at 4, 7, 11, 14, 21, and 28 days after surgery and prepared for histology and immunohistochemical analysis. An additional three animals were sacrificed at 14 days and 28 days after surgery to measure mineral apposition rate (MAR) and bone matrix formation at three different regions of the tunnel.

After sacrifice, the proximal tibias and distal femurs were stripped and harvested. The intra-articular graft was cut to separate the tibia and the femur. The tissues were trimmed and then fixed for 2 days with 10% neutral buffered formalin with 1% cetylpyridinium chloride added to preserve proteoglycans. Each bone tunnel was then divided into three equal sections: intra-articular aperture (IAA), midtunnel (MT), and extra-articular aperture (EAA). The plane of sectioning was perpendicular to the bone tunnel, so that cross-sections of the tendon in the tunnel were made. The first perpendicular cut was made 1 mm below the joint surface to permit evaluation of healing at the

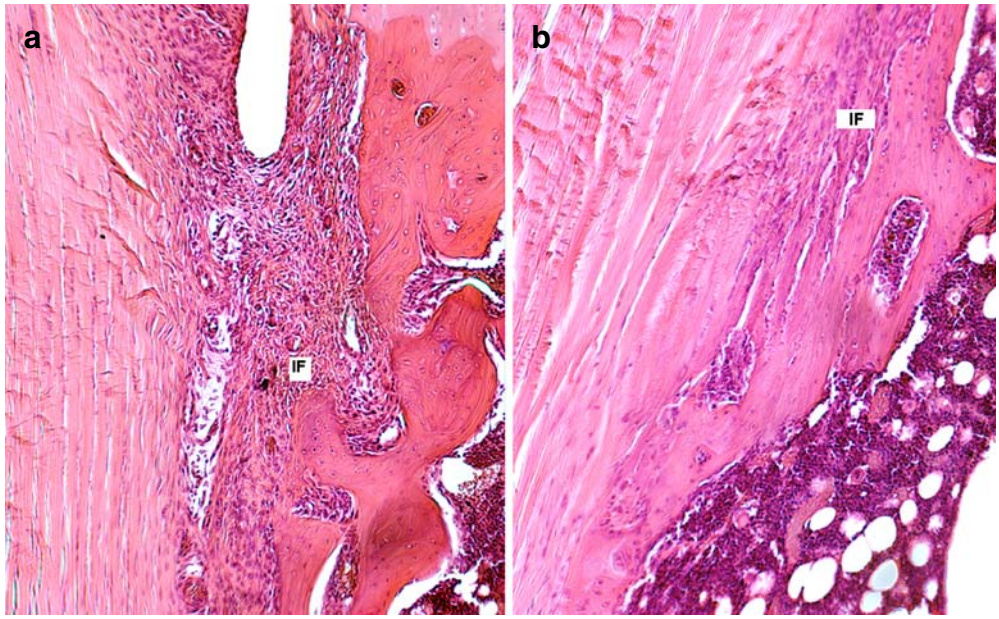

Fig. 1. The morphology of the attachment site of the **a** IAA and **b** EAA at 4 weeks (hematoxylin and eosin staining, ×40 original magnification). The IAA demonstrates a wider tendon–bone interface with loose fibrovascular tissue, while the interface is narrower and more organized at the EAA

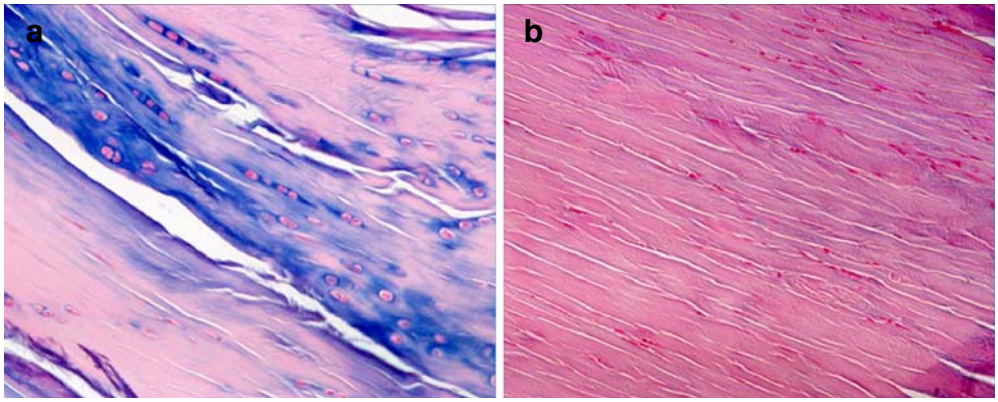

Fig. 2. **a** A more chondroid matrix is seen at the IAA interface (alcian blue staining), compared to the **b** predominantly fibroblastic matrix seen at the mid-tunnel and EAA interface at 4 weeks postoperatively (hematoxylin and eosin staining); ×40 original magnification

IAA but below the articular surface of the knee joint. The tissues were embedded in paraffin and 5 μm thick sections cut in the coronal plane. Staining was performed with hematoxylin and eosin, picrosirius red, and safranin-O. Slides were examined with an Olympus BH-2 light microscope (Olympus Optical Co. Ltd., Tokyo, Japan). Healing between the tendon and the bone was assessed for new tissue formation (fibrovascular granulation tissue, fibrous tissue, cartilage, and bone) between tendon and bone and by narrowing of the tendon–bone interface. We also assessed healing by measuring collagen fiber continuity and orientation between tendon and bone using polarized light microscopy to examine picrosirius-red-stained sections [16, 38]. The illumination and detection parameters of the microscope were kept constant for each specimen to allow direct comparisons.

For immunohistochemical analysis, serial sections were treated with 3% H_2O_2 to quench endogenous peroxidase activity, and nonspecific antibody binding was blocked with 5% goat serum. Bovine serum albumin in phosphate buffered saline (1%) was used as a negative secondary reagent control. The sections were stained using a monoclonal antibody to α-smooth muscle actin (α-SMA), a marker of myofibroblasts and vascular pericytes (Sigma, St. Louis, MO, USA), and NG2 chondroitin sulphate proteoglycan, a marker of immature or progenitor cells (Chemicon, Temecula, CA, USA). The NG2 chondroitin sulfate proteoglycan is expressed by immature progenitor cells in several different developmental lineages, including oligodendrocyte progenitors, chondroblasts, and pericytes/smooth muscle cells [24–29]. Each monoclonal antibody was applied to separate serial sections for 60 min at 37°C, and bound antibodies were visualized using a goat avidin–biotin peroxidase system with 3,3′ diaminobenzidine (DAB, Dako Corp., Carpinteria, CA, USA) as a substrate. Osteoclasts were quantified by chemical staining for tartrate-resistant acid phosphatase activity. The number of osteoclasts and other cells at the tendon–bone interface were counted in ten randomly selected high-power microscopic fields in sections at each of the three regions of the tunnel (EAA, MT, and IAA) [16].

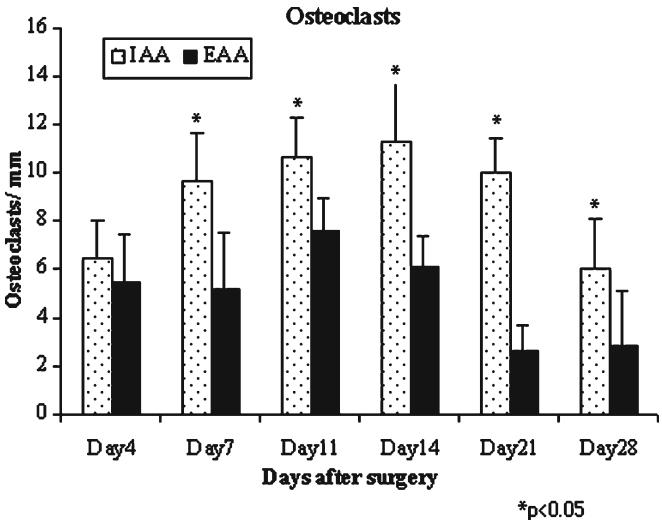

Fig. 3. Significantly increased osteoclasts were noted at the IAA compared to EAA by 1 week after surgery (n=3 animals per group per time point). This difference persisted for the remainder of the 4-week study duration (p<0.05)

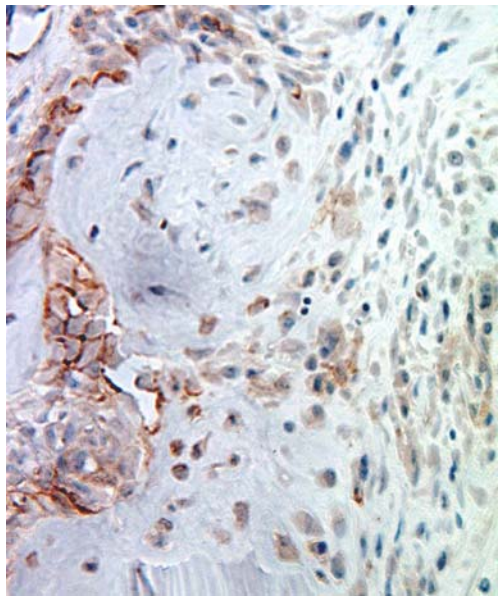

Fig. 4. Immunohistochemical staining for NG2+ cells at 4 weeks. NG2+ cells were localized to the tunnel–graft interface but were not seen in the tendon graft at any time point. ×40original magnification

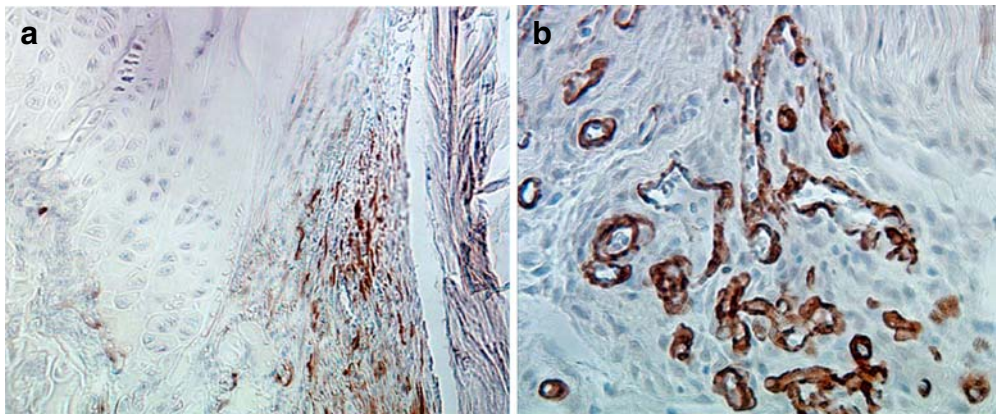

Fig. 5. Immunohistochemical staining of α-SMA+ cells at **a** 4 days and **b** 4 weeks. α-SMA+ positive cells were localized to the healing tendon–bone interface at early time points (**a**) but localized only to mature blood vessels by 4 weeks **(b)**. ×40 original magnification

Mineral apposition rate along the bone tunnel was measured using double fluorochrome labeling techniques. Animals received intraperitoneal injections of calcein (25 mg/kg body weight (BW), Sigma) followed by xylenol orange (90 mg/kg BW, Sigma) 7 and 4 days prior to sacrifice, respectively. Specimens were harvested and embedded in methylmethacrylate without decalcification. Coronal sections (5 μm thick) containing the full length of the tendon graft and bone tunnels were prepared. Alternate sections were stained by the von Kossa and Goldner-Masson trichome method. New bone was detected, and the total area of calcified bone matrix (fraction of total bone area) was measured on the von Kossa-stained histological specimens. Unstained sections were examined on a Nikon Optiphot fluorescence microscope using the Bioquant digitizing system (R&M Biometrics, Nashville, TN, USA). The following primary data were collected from the bone tunnel surface: total perimeter (B.Pm), single-label perimeter (sL.Pm), and double-label perimeter measured along the first label (dL.Pm) and double-label area (dL.Ar). From these primary data, the mineral apposition rate was determined. The MAR reflects the rate at which new bone was deposited in the radial direction [15, 16].

Comparisons in osteoclast counts and MAR were made between the three different tunnel regions and between early and late time points with a two-way analysis of variance, which makes adjustments for multiple comparisons (SPSS Software, Chicago IL, USA). Significance was set at $p<0.05$.

Results

All 24 animals tolerated the procedure well and experienced no postoperative infections or complications. At the time of sacrifice, the reconstructed tendon graft was noted to be intact with tension maintained in all cases. Grossly, the graft appeared securely healed to the bone tunnel by the 2-week sacrifice and for all remaining time points.

Distinct histological differences were evident between the healing enthesis at IAA and EAA by 1 week postoperatively. The IAA had a poorly organized, wide interface tissue between the tendon and bone. In contrast, the EAA demonstrated a more organized and narrow tendon–bone interface (Fig. 1). The interface tissue demonstrated a chondroid matrix at the IAA, whereas the mid-tunnel and EAA interface demonstrated a predominantly fibrous matrix

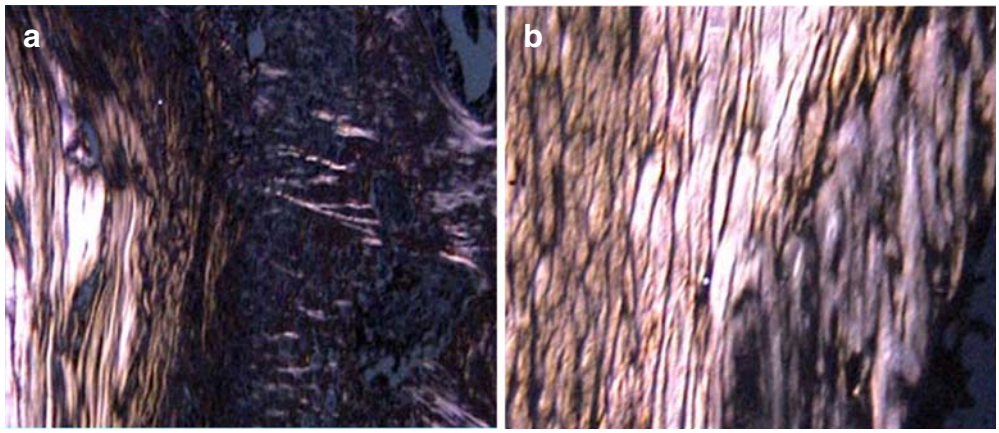

Fig. 6. Collagen fiber orientation between the grafted tendon and bone tunnel at the **a** IAA and **b** EAA at 4 weeks. Fibers demonstrated an organized, parallel orientation at the EAA compared to a less organized, perpendicular orientation at the IAA. Polarization with picrosirius red staining, ×40 original magnification

(Fig. 2). These differences were evident by postoperative day 7 and persisted throughout the remaining study period.

A significantly greater number of osteoclasts were localized to the IAA compared to EAA ($p<0.05$; Fig. 3). Immunostaining for NG2 chondroitin sulphate proteoglycan, a marker for immature progenitor cells and pericytes (24–29), revealed these cells to be predominantly localized to the bone surface at the graft–bone interface (Fig. 4). Localization to the tendon graft was not seen at any time point. No significant differences in NG2 density were appreciated between aperture, mid-tunnel, and exit locations (Fig. 4). Immunostaining for α-SMA, a marker of myofibroblasts and vascular pericytes, revealed localization of these cells to the interface tissue at early time points (<14 days) in all regions of the tunnel (Fig. 5). With progressive maturation of the attachment site, these cells were only seen in the walls of mature blood vessels (>14 days). No significant differences in α-SMA density were appreciated between IAA, mid-tunnel, and EAA sections.

Collagen fiber organization and continuity between the graft and bone tunnel improved over the 4-week period at both the IAA and EAA locations. The density, continuity, and orientation of fibers were consistently different at the EAA compared to IAA by postoperative day 7 and throughout the remaining study period. Orientation was more parallel to the interface at the EAA, while it was orthogonal at the IAA (Fig. 6).

New bone formation as assessed by Goldner-Masson trichrome staining revealed differences between the IAA and EAA location by 2 weeks postoperatively. Quantitative assessment of mineral apposition rate demonstrated successful incorporation of fluorochromes into the newly formed bone around the tendon graft at all three tunnel locations. MAR was significantly higher at the EAA (10.4± 9.6 μm/day) compared with the IAA (5.2±1.9 μm/day) at 4 weeks ($p<0.001$; Fig. 7). Staining of calcified matrix with the von Kossa method confirmed increased mineralization around the tendon graft at all three tunnel locations (IAA, MT, EAA) by 4 weeks compared to 2 weeks after surgery, with no differences between groups.

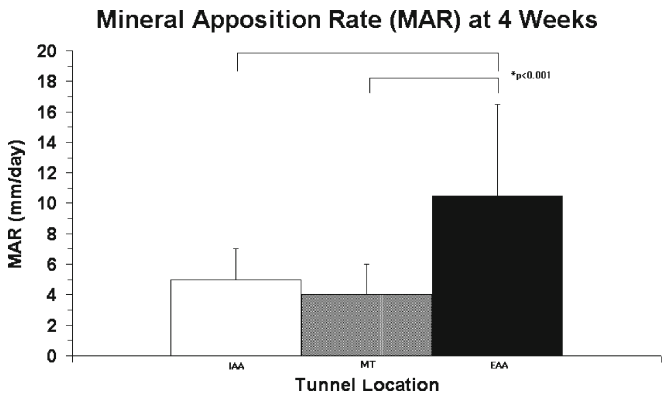

Fig. 7. Mineral apposition rate (*MAR*) of the IAA, mid-tunnel (*MT*), and EAA at 4 weeks. The MAR was significantly less at the IAA and mid-tunnel compared with the EAA at 4 weeks ($p<0.001$)

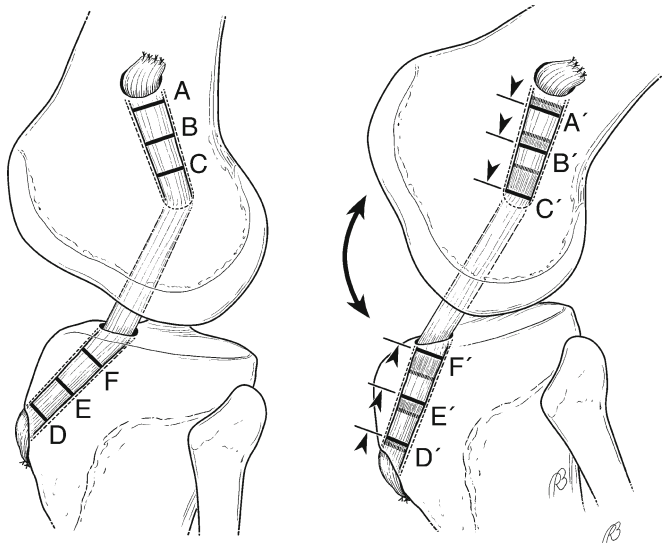

Fig. 8. Effect of increased distance between graft fixation points on graft-tunnel micromotion. "Suspensory fixation" at the EAA of the bone tunnels reduces construct stiffness, increases graft tunnel micromotion, and results in secondary tunnel expansion. The "bungee effect" due to longitudinal graft motion and the "windshield wiper effect" due to transverse motion of the graft in the tunnel may result in distinct differences in the mechanical environment between the IAA and EAA. Note the increased longitudinal motion of the graft at IAA (*C* to *C′* and *F* to *F′*) compared to the EAA (*A* to *A′* and *D* to *D′*) as the distance from the fixation points increase

Discussion

The long-term success of an anterior cruciate ligament reconstruction is ultimately predicated upon the secure healing of tendon to bone. There are no analogous sites in humans where a native tendon passes through a bone tunnel, however, and the biology of this unique environment remains incompletely understood. Wide variations in the morphological characteristics of the tendon–bone attachment site have been reported [5–23]. Some studies have demonstrated formation of a native, direct type of insertion and an intermediate fibrocartilage zone at the interface. In contrast, other studies have reported a fibrous tissue interface with tendon attached to bone by perpendicular collagen bundles [5–23]. Differences in the tendon–bone healing response at different ends of a bone tunnel created during ACL reconstruction, however, have not been characterized.

The current study model demonstrates clear spatial and temporal differences in tendon–bone healing between the intra-articular and extra-articular apertures of a tunnel. The EAA attachment site morphology revealed an organized, fibrous matrix with a narrow tendon–bone interface. Increased collagen fiber continuity from tendon-to-bone oriented in parallel bundles was seen at the EAA. Furthermore, new bone formation and mineral apposition rate were both significantly greater at the extra-articular end of the tunnel by 2 weeks after surgery ($p<0.001$). Significant differences in the number of osteoclasts at different ends of the tunnel were also identified. Osteoclasts were most numerous at the IAA by 7 days after surgery and

throughout the remaining study period ($p<0.05$). The increased quantity of osteoclasts at the IAA may be responsible for the less organized interface morphology and decreased bone formation that was observed relative to the MT and EAA regions.

The etiology of these healing differences detected at the intra-articular versus extra-articular aperture remains unknown, but is likely multifactorial in nature. We hypothesize that differences in the mechanical environment may play a pivotal role. An ACL tendon graft may be fixed with an interference screw in the bone tunnel at the IAA (i.e., aperture fixation) or fixed outside the tunnel at or near the EAA (i.e., suspensory fixation) [16]. Several prior studies have demonstrated a reduction in construct stiffness and secondary increases in graft-tunnel motion with increased distance between fixation points (Fig. 8) [21, 30–36]. Progressively greater graft-tunnel motion occurs as the distance between the fixation point increases, resulting in greater graft-tunnel motion at the tunnel aperture than at the extra-articular end of the tunnel for grafts fixed with suspensory fixation. Such graft-tunnel motion is one possible cause of tunnel widening (Fig. 8) [2, 30, 31, 37].

In our model of ACL reconstruction using suspensory fixation, the impaired graft incorporation and inferior attachment site morphology seen at the IAA may reflect the influence of graft-tunnel micromotion. Prior work from our laboratory in a rabbit ACL reconstruction model using suspensory fixation and radiostereometric analysis supports this hypothesis [10, 16]. Graft tunnel micromotion and tunnel diameter were greatest at the IAA. An inverse correlation between graft-tunnel motion and rate of healing was appreciated, with the slowest healing and widest bone-tunnel interface seen at the IAA [16]. Studies have reported the formation of a direct-type of insertion when ACL graft fixation was performed with an IAA interference screw, while suspensory fixation at the tunnel exit resulted in an indirect insertion [20, 21]. A study that examined delayed biopsies on the healing tendon–bone interface in the femoral tunnel of five patients after ACL reconstruction using hamstring autograft secured with suspensory fixation found loose fibrovascular tissue at the healing tendon–bone interface with minimal collagen fiber continuity between the tendon and bone [10].

Differences in the biological environment at the intra-articular versus extra-articular tunnel apertures may be another critical factor that contributes to the observed histological differences in tendon–bone healing. In our study, staining for immature pericytes and vascular progenitor cells with NG2 and α-SMA did not reveal any appreciable differences between the IAA, MT, or EAA locations. Interestingly, these cells did not repopulate the grafted tendon over the 4-week period. The impaired healing observed at the IAA, however, may reflect the influence of various cytokines or other biological factors that were not assessed in our design. Synovial fluid influx into the bone tunnel is another factor that may affect the healing biology. A study evaluating the healing of empty bone tunnels in rabbit knees found rapid bone formation at the EAA relative to IAA [37]. Rodeo et al. have also suggested a possible inhibitory influence of synovial fluid, reporting a failure of empty bone tunnel healing in a rabbit ACL reconstruction model [16]. The proximity of the physis to the intra-articular aperture may also contribute to the variable healing observed at different regions of the tunnel. While tremendous care was taken to assure that the axial sections at IAA were entirely proximal to the physis, it is possible that displaced physeal cells secondary to drilling of the ACL tunnels may have contributed to variable healing patterns along the length of the tunnel. This is an inevitable limitation of all rodent models, as the physis remains open in these animals despite skeletal maturity and cessation of longitudinal growth. Furthermore, proximity of articular chondrocytes to the IAA or periosteal cells to the EAA may have contributed to differences in the biological environment as well. Furthermore, unrestricted early range-of-motion postoperatively or non-isometric graft positioning are other variables that may have contributed a variable biomechanical environment and the differences observed in tendon–bone healing. Additional studies are needed to evaluate the mechanism underlying the differences observed in this study.

There are several important limitations to our study design. A comparison group of animals reconstructed with aperture fixation would help to assess the influence of biomechanical differences in graft fixation to differences in tendon–bone healing along the tunnel. In addition, histomorphometric analysis at each tunnel region (IAA, MT, and EAA), with quantitative measures of interface tissue width and volume, may have allowed for more objective analysis of differences in healing between each location. Immunohistochemistry for other cell subpopulations (i.e., macrophages and lymphocytes) and cytokines may also have improved our ability to define biological differences at variable regions of the tunnel.

In conclusion, we have found distinct spatial and temporal differences in the graft–bone healing response between the intra-articular and extra-articular apertures of a bone tunnel in an ACL reconstruction model using suspensory fixation. Healing at the extra-articular aperture demonstrates improved collagen fiber continuity, orientation, and new bone formation relative to the intra-articular entrance by 4 weeks. A relative accumulation of osteoclasts occurs at the intra-articular aperture and may be responsible for the slower healing response and diminished formation of new bone at this location. This disparity in healing and osteoclast activity likely reflects differences in the local biomechanical and biological environment at each end of the tunnel.

References

1. Ishibashi Y, Rudy TW, Livesay GA, Stone JD, Fu FH, Woo SL (1997) The effect of anterior cruciate ligament graft fixation site at the tibia on knee stability: evaluation using a robotic testing system. Arthroscopy 13:177–182
2. Otsuka H, Ishibashi Y, Tsuda E, Sasaki K, Toh S (2003) Comparison of three techniques of anterior cruciate ligament reconstruction with bone–patellar tendon–bone graft: differences in anterior tibial translation and tunnel enlargement with each technique. Am J Sports Med 31:282–288

3. Scheffler SU, Sudkamp NP, Gockenjan A, Hoffmann RF, Weiler A (2002) Biomechanical comparison of hamstring and patellar tendon graft anterior cruciate ligament reconstruction techniques: the impact of fixation level and fixation method under cyclic loading. Arthroscopy 18:304–315
4. Tsuda E, Fukuda Y, Loh JC, Debski RE, Fu FH, Woo SL (2002) The effect of soft-tissue graft fixation in anterior cruciate ligament reconstruction on graft-tunnel motion under anterior tibial loading. Arthroscopy 18:960–967
5. Blickenstaff KR, Grana WA, Egle D (1997) Analysis of a semitendinosus autograft in a rabbit model. Am J Sports Med 25:554–559
6. Chiroff RT (1975) Experimental replacement of the anterior cruciate ligament: a histological and microradiographic study. J Bone Joint Surg Am 57:1124–1127
7. Grana WA, Egle DM, Mahnken R, Goodhart CW (1994) An analysis of autograft fixation after anterior cruciate ligament reconstruction in a rabbit model. Am J Sports Med 22:344–351
8. Kjaer M (2004) Role of extracellular matrix in adaptation of tendon and skeletal muscle to mechanical loading. Physiol Rev 84:649–698
9. Liu SH, Panossian V, Al-Shaikh R et al (1997) Morphology and matrix composition during early tendon to bone healing. Clin Orthop Relat Res 339:253–260
10. Nebelung W, Becker R, Urbach D, Ropke M, Roessner A (2003) Histological findings of tendon–bone healing following anterior cruciate ligament reconstruction with hamstring grafts. Arch Orthop Trauma Surg 123:158–163
11. Panni AS, Milano G, Lucania L, Fabbriciani C (1997) Graft healing after anterior cruciate ligament reconstruction in rabbits. Clin Orthop Relat Res 343:203–212
12. Peterson W, Laprell H (2000) Insertion of autologous tendon grafts to the bone: histological and immunohistochemical study of hamstring and patellar tendon graft. Knee Surg Sports Traumatol Arthrosc 8:26–31
13. Pinczewski LA, Clingeleffer AJ, Otto DD, Bonar SF, Corry IS (1997) Integration of hamstring tendon graft with bone in reconstruction of the anterior cruciate 997 ligament. Arthroscopy 13:641–643
14. Rodeo SA, Arnoczky SP, Torzilli PA, Hidaka C, Warren RF (1993) Tendon-healing in a bone tunnel. J Bone Joint Surg Am 75:1795–1803
15. Rodeo SA, Suzuki K, Deng XH, Wozney J, Warren R (1999) Use of recombinant human bone morphogenetic protein-2 to enhance tendon healing in a bone tunnel. Am J Sports Med 27:476–488
16. Rodeo SA, Kawamura S, Kim HJ, Dynybil C, Ying L (2006) Tendon healing in a bone tunnel differs at the tunnel entrance versus the tunnel exit: an effect of graft-tunnel motion. Am J Sports Med 34:1790–800
17. Sakai H, Fukui N, Kawakami A, Kurosawa H (2000) Biological fixation of the graft within bone after anterior cruciate ligament reconstruction in rabbits: effects of the duration of postoperative immobilization. J Orthop Sci 5:43–51
18. St Pierre P, Olson EJ, Elliott JJ, O'Hair KC, McKinney LA, Ryan J (1995) Tendon healing to cortical bone compared with healing to a cancellous tough: a biomechanical and histological evaluation in goats. J Bone Joint Surg Am 77:1858–1866
19. Thomopoulos S, Williams GR, Soslowsky LJ (2003) Tendon to bone healing: differences in biomechanical, structural, and compositional properties due to a range of activity levels. J Biomech Eng 125:106–113
20. Weiler A, Hoffmann RF, Bail HJ, Rehm O, Sudkamp NP (2002) Tendon healing in a bone tunnel, part II: histologic analysis after biodegradable interference fit fixation in a model of anterior cruciate ligament reconstruction in sheep. Arthroscopy 18:124–135
21. Weiler A, Unterhauser FN, Faensen B, Hunt P, Bail HJ, Haas NP (2002) Comparison of tendon-to-bone healing using extracortical and anatomic interference fit fixation of soft tissue grafts In a sheep model of ACL reconstruction. Trans Orthop Res Soc 27:173
22. Yoshiya S, Nagano M, Kurosaka M, Muratsu H, Mizuno K (2000) Graft healing in the bone tunnel in anterior cruciate ligament reconstruction. Clin Orthop Relat Res 376:278–286
23. Burg M, Pasqualini R, Arap W, Ruoslahti E, Stallcup W (2000) NG2 proteoglycan-binding peptides target tumor neovasculature. Cancer Res 59:2869–2874
24. Grako KA, Ochiya T, Barritt D, Nishiyama A, Stallcup W (1999) PDGF a-receptor is unresponsive to PDGF-AA in aortic smooth muscle cells from the NG2 knockout mouse. J Cell Sci 112:905–915
25. Grako KA, Stallcup W (1995) Participation of NG2 proteoglycan in rat aortic smooth muscle cell responses to platelet-derived growth factor. Exp Cell Res 221:231–240
26. Nishiyama A, Dahlin K, Stallcup W (1991) The expression of NG2 proteoglycan in the developing rat limb. Development 111:933–944
27. Schlingemann R, Rietveld F, de Waal R, Ferrone S, Ruiter D (1990) Expression of the high molecular weight melanoma-associated antigen by pericytes during angiogenesis in tumors and in healing wounds. Am J Pathol 136:1393–1405
28. Schlingemann R, Oosterwijk E, Wesseling P, Rietveld F, Ruiter D (1996) Aminopeptidase A is a constituent of activated pericytes in angiogenesis. J Pathol 179:436–442
29. Barber FA, Spruill B, Sheluga M (2003) The effect of outlet fixation on tunnel widening. Arthroscopy 19:485–492
30. Clatworthy MG, Annear P, Bulow JU, Bartlett RJ (1999) Tunnel widening in anterior cruciate ligament reconstruction: a prospective evaluation of hamstring and patella tendon grafts. Knee Surg Sports Traumatol Arthrosc 7:138–145
31. Hantes ME, Mastrokalos DS, Yu J, Paessler HH (2004) The effect of early motion on tibial tunnel widening after anterior cruciate ligament replacement using hamstring tendon grafts. Arthroscopy 20:572–580
32. Hoher J, Livesay GA, Ma CB, Withrow JD, Fu FH, Woo SL (1999) Hamstring graft motion in the femoral bone tunnel when using titanium button/polyester tape fixation. Knee Surg Sports Traumatol Arthrosc 7:215–219
33. Hoher J, Moller HD, Fu FH (1998) Bone tunnel enlargement after anterior cruciate ligament reconstruction: fact or fiction. Knee Surg Sports Traumatol Arthro 6:231–240
34. Sidles JA, Clark JM, Garbini JL (1991) A geometric theory of the equilibrium mechanics of fibers in ligaments and tendons. J Biomech 24:943–949
35. Simonian PT, Erickson MS, Larson RV, O'kane JW (2000) Tunnel expansion after hamstring anterior cruciate ligament reconstruction with 1-incision EndoButton femoral fixation. Arthroscopy 16:707–714
36. L'Insalata JC, Klatt B, Fu FH, Harner CD (1997) Tunnel expansion following anterior cruciate ligament reconstruction: a comparison of hamstring and patellar tendon autografts. Knee Surg Sports Traumatol Arthrosc 5:234–238
37. Berg EE, Pollard ME, Kang Q (2001) Interarticular bone tunnel healing. Arthroscopy 17:189–195
38. Noorlander ML, Melis P, Jonker A, Van Noorden CJF (2002) A quantitative method to determine the orientation of collagen fibers in the dermis. J Histolochem Cytochem 50(11):1469–1474